



HAL
open science

Small-scale demonstrator of a cold thermal store for liquid air energy storage

Alain Damas, Daniele Negro, Denis Leducq, Anthony Dallais, Graciela Alvarez,
Tim Brown, Judith Evans, Alan Foster

► **To cite this version:**

Alain Damas, Daniele Negro, Denis Leducq, Anthony Dallais, Graciela Alvarez, et al.. Small-scale demonstrator of a cold thermal store for liquid air energy storage. 6th IIR Conference on Sustainability and the Cold Chain, Aug 2020, NANTES, France. <10.18462/iir.iccc.2020.295155>. <hal-03367980>

HAL Id: hal-03367980

<https://hal.science/hal-03367980v1>

Submitted on 6 Oct 2021

HAL is a multi-disciplinary open access archive for the deposit and dissemination of scientific research documents, whether they are published or not. The documents may come from teaching and research institutions in France or abroad, or from public or private research centers.

L'archive ouverte pluridisciplinaire **HAL**, est destinée au dépôt et à la diffusion de documents scientifiques de niveau recherche, publiés ou non, émanant des établissements d'enseignement et de recherche français ou étrangers, des laboratoires publics ou privés.



HAL Authorization

Small-scale demonstrator of a cold thermal store for liquid air energy storage

Alain DAMAS^(a), Daniele NEGRO^(b), Denis LEDUCQ^(c), Antony DALLAIS^(a), Graciela ALVAREZ^(c), Tim BROWN^(b), Judith EVANS^(b), Alan FOSTER^(b)

^(a) Air Liquide

Paris, 78350, France, alain.damas@airliquide.com

^(b) London South Bank University

Langford, BS40 5DU, UK, alan.foster@lsbu.ac.uk

^(c) INRAE

Antony, 92160, France, graciela.alvarez@irstea.fr

1. ABSTRACT

Intermittency of renewable energy supply causes an issue for grid balancing, as electricity generation is not easily controllable. A method to balance power supply and demand is to store energy during low-demand periods and use it at high demand.

Cryogenic energy storage (CES) uses liquefied gas as an energy storage and transfer medium. Recycling cold from the expansion to the liquefier is a way to boost the CES efficiency. As the cold release from the evaporation of cryogen happens at a different time than the gas liquefaction, such an exchange of low-temperature energy requires a thermal store.

A small-scale demonstrator of a packed-bed cold thermal store for use in LAES, integrated with a refrigerated warehouse, was built and run under different thermo-hydraulic conditions. It was able to store 2.92 kWh with round trip efficiency of up to 0.650 when storing for 1 hour and 0.490 when storing for 24 hours.

Keywords: Thermal store, Liquid Air Energy Storage (LAES), thermocline, packed bed.

2. INTRODUCTION

The EU has already met its 2020 renewable energy target (Renewable energy directive 2009/28/EC) of 20% final energy consumption from renewable sources by 2020. By 2030 the revised Renewable Energy Directive (2018/2001) established a new binding renewable energy target for the EU for 2030 of at least 32%. As the EU and the rest of the world moves towards even more renewable energy, supply becomes more dependent on factors outside the control of the energy supplier, e.g. weather variations. This causes an issue for grid balancing, as renewable electricity generation is not easily controllable. One method to balance supply and demand in power generation is to store energy during periods of low demand and use it at high demand. Lehmann et al. (2016) stated that “The UK can realise significant cost savings if market arrangements for the electricity system allow for an efficient deployment and use of energy storage...”

For renewable generation to take a larger share of the energy market, as required by climate targets, energy storage will become more necessary. According to Barton and Infield (2004) short-term storage, covering less than 1 hour, offers only a small increase in the amount of electricity that can be absorbed by the network. Storage over periods of up to one day delivers greater energy benefits but is significantly more expensive. According to Roberts (2018) “We have the storage technology to smooth out hourly swings, but we still don’t have anything that could cover a fallow period of wind and sun that lasted days, months, or even years. If we want to get variable renewable energy up to 60 percent, 80 percent, or even more of our electricity, we need long-term energy storage. It is the missing puzzle piece, the holy grail.”

Current technology, e.g. batteries, are not a cost-effective solution for long term storage as the cost scales linearly with energy capacity. Pumped hydro and compressed air (CAES) are not easily deployable due to their geographical and geological requirements. Cryogenic energy storage (CES) makes use of low-temperature liquids as an energy storage and transfer medium. CES can provide large-scale, long-duration energy storage of 5 to 1000 MWh (Brett and Barnett, 2014). The use of liquid air to store energy, which can then be recovered as mechanical work, dates back to 1900, when the Tripler Liquid Air Company developed a

liquid air car.

One of the current issues with CES is its low round trip efficiency (RTE, the ratio of energy recovered to energy in) compared with pumped hydro electrical storage, compressed air energy storage and Li-ion batteries.

A liquid air energy storage system has been demonstrated by Highview Power Storage (Morgan et al., 2015). They showed that the RTE could be greatly increased by recycling more of the cold from the expansion to the liquefier. The generation of cold from the expansion turbines happens at a different time than the liquefaction of the air. For this reason, the cold energy to be exchanged requires a thermal store. Morgan et al. (2015) used a bed of quartzite gravel beads contained inside a shipping container to store the cold energy. They only managed to recycle 51% of their cold energy in their pilot scale plant. They stated that over 50% RTE would be achievable if the percentage of cold recycling increased from 51% to 91% and the process was optimised to maximise cooling from adiabatic expansion.

Peng et al. (2018) conducted an analysis of a LAES with packed beds. They concluded that the system could achieve an RTE in the range 50–62% depending on the values of process conditions and that this is a bit lower than a CAES. However, the storage energy density is much higher for the same operational conditions.

Sciacovelli et al, 2017 modelled a LAES with packed bed thermal storage. They found that the temporary storage of cold thermal energy streams using packed beds improves efficiency of LAES by ~50%. However, due to dynamic cycling charge/discharge, packed beds can bring an undesired 25% increase in the energy expenditure needed to liquefy air.

The aim of this study was to evaluate the thermal capacity and efficiency of a small-scale demonstrator packed bed thermal store.

3. METHOD

The thermal tank was a cylindrical container, 0.840 m high, with an internal diameter of 0.451 m and 3 mm thick stainless-steel walls. The tank was insulated with 200 mm polyisocyanurate (PIR) (ISOPIRFLAM33®). The height of the heat storage material (HSM) in the tank was 600 mm. The total bed volume was 0.959 m³.

The HSM was 3.25 mm mean diameter polished soda-lime glass spheres, composed of 72% silicon dioxide (SiLibeads® Type S, SIGMUND LINDNER GmbH). They had a specific weight of 2.5 kg.l⁻¹, roundness >0.95 and thermal conductivity of 1.129 W.m⁻¹.K⁻¹. Using the thermal properties of pure silica, the heat capacity of the glass beads at varied temperatures was calculated using the Cryogenic Material Properties Database provided by Marquardt et al (2002).

The thermal store was filled with 146.7 kg of HSM with 39% porosity. This gave a bed aspect ratio (height/diameter) of 1.33.

Liquid nitrogen was evaporated before being fed into the thermal tank. Therefore, only gaseous nitrogen entered the tank.

3.1. Instrumentation

The mean temperature of the HSM was measured using T-type thermocouples at the axial centre and edge of the cylinder at 6 regularly spaced heights. The central thermocouples were held by wire and the edge thermocouples were inserted into the wall of the thermal store.

The thermocouples were calibrated at temperatures which coincided with melting ice, CO₂ triple point and the boiling point of N₂ at atmospheric pressure.

Flow rate of nitrogen was measured by a turbine volumetric flowmeter (Hoffer Flow Controls HIT-2A). Pressure and temperature measurement close to the flowmeter was recorded to convert volumetric flow rate into mass flow rate.

The weight of the liquid nitrogen tank was measured using 3 load cells (METTLER TOLEDO RLC) that provided real time weight measurement and cross checked information against the flowmeter.

3.2. Stages of operation

The thermal store operation was split into 3 separate stages;

Charge – To extract heat from the HSM using the cold nitrogen, thus storing cold energy.

Storage – Maintaining the temperature of the HSM between charging and discharging.

Discharge – To cool nitrogen entering the HSM by exchanging heat with the cold HSM thus releasing cold energy.

As nitrogen passed through the HSM a thermozone was generated. During the dynamic phases (charge and

discharge), the total temperature swing was defined by Eq. (1)

$$\Delta T_{max} = T_{hot} - T_{cold} \quad \text{Eq. (1)}$$

Where T_{hot} and T_{cold} were the maximum and minimum temperature of the fluid recorded in the test.

During charging, nitrogen gas was driven to the store and entered at the bottom of the tank and exited at the top. Charge cycles were performed and repeated with various flow rates and ΔT_{max} . Charging was performed until “breakthrough”. Breakthrough was defined as the time when the fluid temperature at exit of the tank was equal to T_{bt} as shown in Eq. (2).

$$T_{bt} = T_{cold} + 0.1 \cdot \Delta T_{max} \quad \text{Eq. (2)}$$

In some cases this condition was not achieved, in which case breakthrough was considered as the time when temperature difference between the top and bottom was less than 1 K.

A total of 6 storage sequences were performed between charge and discharge, two were long periods (18 hours and 28 hours) and 4 were short storage periods (approximately 2 hours). There was no flow of nitrogen through the HSM during the storage stage.

During discharge, nitrogen at ambient temperature was input at the top of the store and cold nitrogen exited at the bottom.

The tests followed the following sequence; charge followed by storage followed by discharge. Before charging, the vessel was at ambient temperature.

3.3 Efficiency

During charging, the energy input of the fluid into the thermal store was as shown in Eq. (3).

$$E_{charge} = \dot{m} \int_{t=0}^{t=breakthrough} (h_i - h_o) dt \quad \text{Eq. (3)}$$

Where, \dot{m} , was the mass flow rate of the nitrogen, h_i and h_o , were the enthalpy of the nitrogen entering and exiting the store respectively (calculated from REFPROP) and t , was time the time step of 1 s.

The energy stored in the bed is shown in Eq. (4).

$$E_{stored} = m_s \int_{T_1}^{T_2} c_p (T) \cdot dT \quad \text{Eq. (4)}$$

Where m_s was the mass of the HSM and C_p is specific heat at the mean temperature, T was the temperature of the HSM.

The charge efficiency was defined as the ratio of energy stored and supplied shown in Eq. (5)

$$\mu_c = \frac{E_{stored}}{E_{charged}} \quad \text{Eq. (5)}$$

During discharging, the energy removed from the fluid as it exited the thermal store was calculated in the same way as shown in Eq. (3).

The discharge efficiency was defined as the ratio of energy discharged and stored as shown in Eq. (6)

$$\mu_d = \frac{E_{discharged}}{E_{stored}} \quad \text{Eq. (6)}$$

The storage efficiency was defined as shown in Eq. (7)

$$\mu_s = \frac{E_{stored2}}{E_{stored1}} \quad \text{Eq. (7)}$$

Where $E_{stored1}$ was the energy stored in the HSM and $E_{stored2}$ was the energy at the end of the storage time.

The round trip efficiency, μ_{RTE} of the storage vessel could be calculated using Eq. (8)

$$\mu_{RTE} = \mu_c \cdot \mu_d \cdot \mu_s \quad \text{Eq. (8)}$$

4. RESULTS

4.1. Charging

When charging was started, the inlet temperature was not instantaneously at the coldest temperature due to an initial lag time. The dimensionless inlet temperature evolution $T_{\text{dim-bottom}}$ (Eq. (9)) with time is shown in Figure 1a and dimensionless outlet temperature evolution $T_{\text{dim-top}}$ (Eq. (10)) with time is shown in Figure 1b. There was a temporary problem with data acquisition, hence the gap in data at 18.5 g/s in Figure 1a.

$$T_{\text{dim-bottom}} = (T_{\text{bottom}} - T_{\text{cold}}) / \Delta T_{\text{max}} \quad \text{Eq. (9)}$$

$$T_{\text{dim-top}} = (T_{\text{top}} - T_{\text{cold}}) / \Delta T_{\text{max}} \quad \text{Eq. (10)}$$

It took between 340 and 1900 s before $T_{\text{dim-bottom}}$ reached 0.1. It took over 1800 s for $T_{\text{dim-top}}$ to reach 0.9 and between 2700 and 8500 s to reach 0.1. Not surprisingly the higher flow rate of nitrogen caused a faster reduction in temperature.

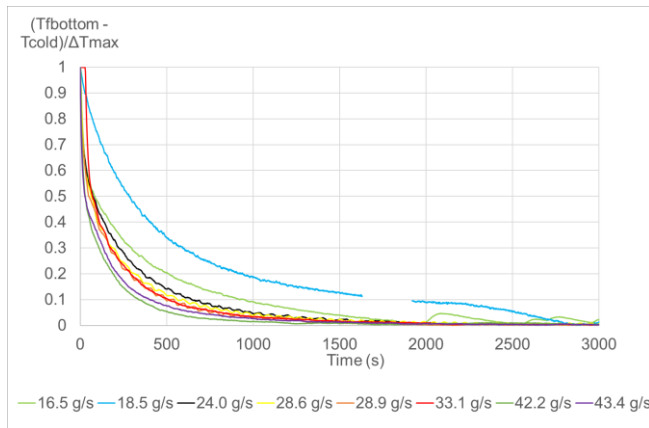


Figure 1a. Inlet fluid dimensionless temperature history for different flow rates during charge.

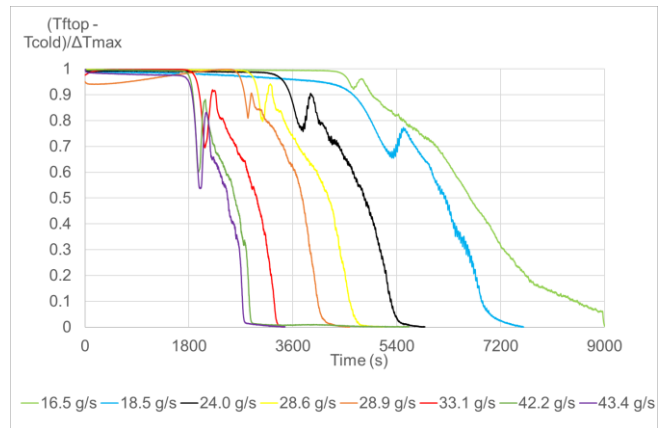


Figure 1b. Outlet fluid dimensionless temperature history for different flow rates during charge.

4.2. Storage

Figure 2a and Figure 2b show mean temperature evolution of the HSM recorded during short and long storage periods respectively.

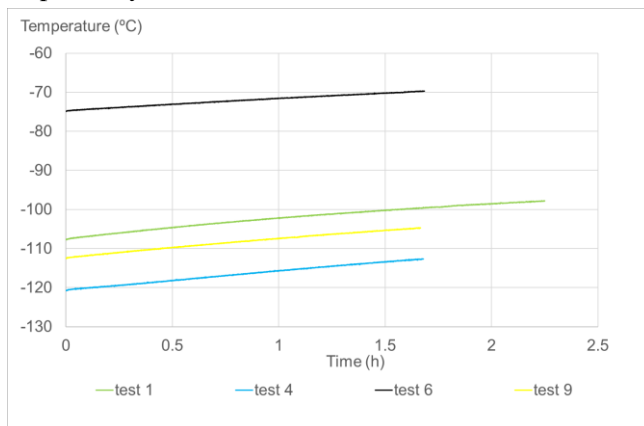


Figure 2a. Mean bed temperature evolution during short term storage.

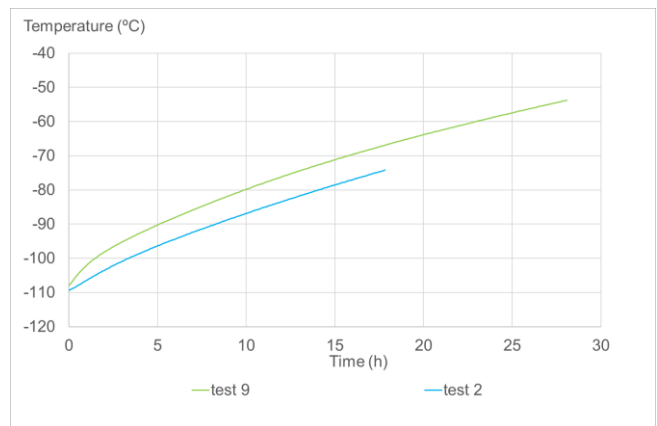


Figure 2b. Mean bed temperature evolution during long term storage.

4.3. Discharge

During discharge the dimensionless inlet temperature evolution with time is shown in Figure 3a and dimensionless outlet temperature evolution with time is shown in Figure 3b. When discharge was started, $T_{\text{dim-top}}$ was approximately

0.5. It took between 300 and 630 s before $T_{\text{dim-top}}$ reached 0.9. It took between 4800 and 9600 s before $T_{\text{dim-bottom}}$ reached 0.9. Not surprisingly the higher flow rate of nitrogen caused a faster increase in temperature.

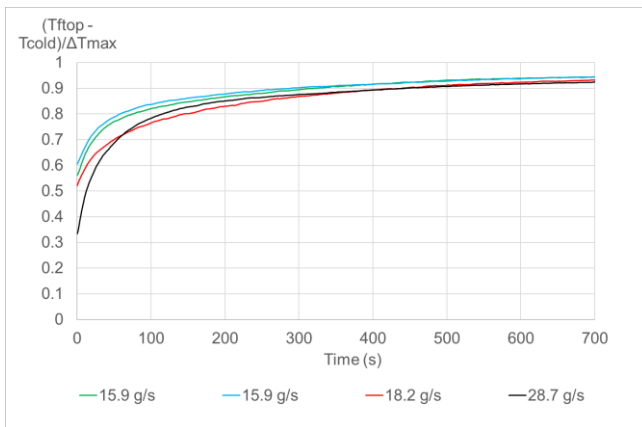


Figure 3a. Inlet fluid dimensionless temperature history for different flow rates during discharge.

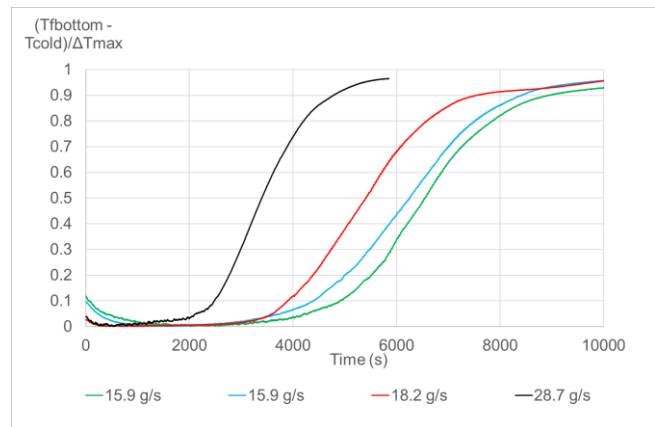


Figure 3b. Outlet fluid dimensionless temperature history for different flow rates during discharge

4.4 Efficiency

Table 1 shows the efficiency and energy stored during charging for the different tests. Results for charging when a thermocline was present within the storage vessel ($T_{\text{dim-top}} = 0.9$) and when there was no thermocline (charging until all vessel was at approximately the same temperature) ($T_{\text{dim-top}} = 0.1$) are given. The energy stored was obviously higher (by around 20%) when $T_{\text{dim-top}} = 0.1$ with a mean value of 2.92 kWh compared to 2.43 kWh. Efficiency was compromised when $T_{\text{dim-top}} = 0.1$, with a mean value of 82.2% compared to 89.7%, an efficiency reduction of 7.6%.

Table 1. Efficiency and energy stored in the charging process.

Flow rate (g/s)	ΔT_{max} (K)	$T_{\text{dim-top}} = 0.9$		$T_{\text{dim-top}} = 0.1$	
		Energy stored (kWh)	Efficiency	Energy stored (kWh)	Efficiency
16.5	134	2.57	89.3	3.15	78.3
24	97	1.97	90.0	2.41	81.9
28.5	131	2.61	84.9	3.12	83.9
28.9	120	2.35	90.8	2.82	82.6
33.1	131	2.52	90.3	3.04	80.3
42.3	138	2.69	91.6	3.18	83.4
43.4	126	2.44	91.2	2.94	84.8
Mean		2.43	89.7	2.92	82.2

The storage efficiency, μ_s , reduced with time due to heat transfer from the ambient. Short term storage had a greater reduction in efficiency with time with a mean of 2.4% per hour, whereas long term storage was 1.1% per hour. This was due to the rate of heat loss reducing with time as the vessel approached ambient temperature.

Results are only presented for discharging, leaving the thermocline within the vessel ($T_{\text{dim-bottom}} = 0.1$), as the thermocline was considered too warm to have practical value. A mean energy recovered of 2.10 kW and efficiency of 74.2% was measured.

The μ_{RTE} calculated depends on whether the thermocline remained in the HSM during charging and the length of storage. Assuming the thermocline remained in the HSM, after a storage time of 1 hour an μ_{RTE} of $(0.897 \times 0.976 \times 0.742)$ 0.650 was achieved, based on the mean values for the tests conducted. If the thermocline was passed through the thermal store during charging, increasing the storage capacity, the μ_{RTE} dropped to 0.596. For storage periods of 24 hours, the storage efficiency was 0.736. This reduced the μ_{RTE} to 0.490 when the thermocline was present and 0.449 when the thermocline was not present in the HSM. Results are only presented for discharging, leaving the thermocline within the vessel ($T_{\text{dim-bottom}} = 0.1$), as the thermocline was considered too warm to have practical value. A mean energy recovered of 2.10 kW and efficiency of 74.2% was measured.

Table 2 shows the efficiency and energy recovered during discharging for the different tests. Results are only presented for discharging, leaving the thermocline within the vessel ($T_{\text{dim-bottom}} = 0.1$), as the thermocline was considered too warm to have practical value. A mean energy recovered of 2.10 kW and efficiency of 74.2% was measured.

Table 2. Efficiency and energy stored in the discharging process.

		$T_{\text{dim-bottom}} = 0.1$	
Flow rate (g/s)	ΔT_{max} (K)	Energy recovered (kWh)	Efficiency
15.9	84	1.74	75.8
15.9	117	2.22	72.9
18.2	126	2.17	72.3
28.7	121	2.26	75.8
mean	112	2.10	74.2

6. CONCLUSIONS

A thermal store was built and tested to ascertain the efficiency of storing cold from gaseous nitrogen, evaporated from cryogenic temperatures. The thermal store was able to store 2.43 kWh at high efficiency and 2.92 kWh at low efficiency. The round trip efficiency of the thermal store ranged between 0.596 and 0.650 when storing for 1 hour and 0.490 and 0.449 when storing for 24 hours.

7. ACKNOWLEDGEMENTS

The CryoHub project has received funding from the European Union's Horizon 2020 Research and Innovation Programme under Grant Agreement No 691761.

REFERENCES

- Barton, J.P., Infield, D.G., 2004. Energy Storage and its Use with Intermittent Renewable Energy. IEEE T. E. Conv.
- Brett, G., Barnett, M., 2014. The application of liquid air energy storage for large scale long duration solutions to grid balancing. Highview Power Storage, London, UK.
- Lehmann, N., Lever, A., Sanders, D., Ravishankar, M., Ashcroft, M., 2016. Can storage help reduce the cost of a future UK electricity system. The Carbon Trust.
- Marquardt, E.D., Le J.P., Radebaugh R., 2002. Cryogenic Material Properties Database. In: Ross R.G. (eds) Cryocoolers 11. Springer, Boston, MA.
- Morgan, R., Nelmes, S., Gibson, E., Brett, G., 2015. Liquid air energy storage—analysis and first results from a pilot scale demonstration plant. Appl. Energ. 137, 845-853.
- Peng, H., Shan, X., Yang, Y., Ling, X., 2018. A study on performance of a liquid air energy storage system with packed bed units. Appl. Energ. 211, 126–135.
- Renewable Energy Directive, 2009. Directive 2009/28/EC of the European parliament and of the council of 23 April 2009 on the promotion of the use of energy from renewable sources and amending and subsequently repealing Directives 2001/77/EC and 2003/30/EC. Official Journal of the European Union.
- Renewable Energy Directive, 2018. Directive (EU) 2018/2001 of the European parliament and of the council of 11 December 2018 on the promotion of the use of energy from renewable sources. Official Journal of the European Union.
- Roberts, 2018., A tiny, beleaguered government agency seeks an energy holy grail: long-term energy storage. <https://www.vox.com/energy-and-environment/2018/9/20/17877850/arpa-e-long-term-energy-storage-days>.
- Sciakovelli, A., Vecchi, A., Ding, Y., 2017. Liquid air energy storage (LAES) with packed bed cold thermal storage - From component to system level performance through dynamic modelling, Appl. Energ., 190, 84-9.